



Gamma-ray shielding studies on borate glasses containing BaO, Bi₂O₃, and PbO in different concentrations

Reza Bagheri ^{a,*}, Seyed Pezhman Shirmardi ^b

^a Northwest Research Complex (Bonab), Radiation Applications Research School, Nuclear Science and Technology Research Institute, Tehran, Iran

^b Radiation Applications Research School, Nuclear Science and Technology Research Institute, Tehran, Iran



ARTICLE INFO

Keywords:
 Borate glass
 Mass attenuation coefficient
 Effective atomic number and electron density
 MCNPX
 XCOM
 XMuDat

ABSTRACT

Mass attenuation coefficients (μ_m), half value layer (HVL), effective atomic cross sections (σ_a), effective atomic numbers (Z_{eff}) and effective electron densities (N_{eff}) of borate glasses containing different concentrations of BaO, Bi₂O₃, and PbO (20–50% by mole) were obtained in the energy range of 10 keV–10 MeV using MCNPX code, XCOM and XMuDat programs, Auto-Z_{eff} software and linear interpolation method. The simulated and calculated results were in good agreement with the experimental data with differences of $\leq \pm 11\%$. It was found that σ_a and Z_{eff} of glass samples improve by increasing their BaO, PbO and Bi₂O₃ contents, while increasing these contents to the same fraction has no significant effect on μ_m values in the energy range of 0.3–6 MeV, where the Compton Effect takes over as dominant process. In addition, the μ_m and σ_a values of glasses decreased with photon energy and bismuth oxide borate glass obtained the highest values of μ_m and σ_a . Also, HVL values of the studied glasses decreased with the increase in their densities. The 50Bi₂O₃:50B₂O₃ glass system had the highest Z_{eff} value of 55.60 at the 30 keV photon energy. Above 0.4 MeV photon energy, N_{eff} values were independent of the metal oxides contents. The N_{eff} values of the studied glass systems varied in the range of $2.77 \times 10^{23} – 9.10 \times 10^{23}$ electron/g.

1. Introduction

With the increasing usage of gamma rays in industry, agriculture and medicine, protection against them is essential. However concretes and lead bricks and sheets are the most common radiation shielding materials, but they have some mechanical, chemical, optical and toxicological disadvantages (Singh et al., 2013; Akkurt and Tekin, 2020; Obaid et al., 2018a, b). This has led researchers to work on other materials such as glasses.

Glass materials due to the 100% recyclability, transparency to visible light, property modifiability through adding different metal oxides and so on, are a good option for this purpose (Bagheri et al., 2017a; Yasmin et al., 2018; Saddeek et al., 2020). Various types of glasses have been studied in nuclear-related applications. Extensive theoretical and experimental works were done on the silicate, tellurite, borosilicate, phosphate and germanium based glasses containing different concentration of heavy metal oxides such as Bi₂O₃, PbO, BaO, ZnO, Nb₂O₅, TiO₂, MgO, Ag₂O, Cr₂O₃, Sb₂O₃ and so on (Kirdsiri et al., 2011; Al-Hadeethi et al., 2020a, b, c; Bagheri and Adeli, 2020; Kaky et al., 2020; Susoy et al., 2020; Sayyed et al., 2018; Tekin et al., 2020a, b).

In the present work, borate based glasses have been considered for investigation. These glasses are well known for their distinctive features such as thermal stability, low melting point, good transparency to visible light, low cost, ease preparation, and excellent solvent performance for metal oxides for shielding purposes (Al-Buriabi et al., 2020; Sayyed et al., 2019). Although, several sporadic studies were conducted on borate based glasses by adding light and heavy elements like lithium, sodium, magnesium, lanthanum, zinc, Tungsten, barium, lead, and bismuth (Abouhaswa et al., 2020; Sayyed et al., 2020a, b; Kumar et al., 2020), but no one has specifically studied the effect of all three of BaO, Bi₂O₃, and PbO heavy metal oxides on gamma ray shielding of borate glasses solely at the wide energy range of 1 keV–10 MeV. In addition to the stabilization of glass structure and improvement of chemical durability (Bagheri et al., 2018), addition of heavy elements to the borate glass frame, dramatically improve their radiation attenuation feathers.

In this study, three borate glass systems, namely xBi₂O₃:(100-x)B₂O₃, xPbO:(100-x)B₂O₃, and xBaO:(100-x)B₂O₃ glasses (where $20 \leq x \leq 50$ is expressed in terms of mol%) were considered. The mass attenuation coefficients, half value layer, effective atomic cross section, effective atomic number and electron density values of borate glasses were

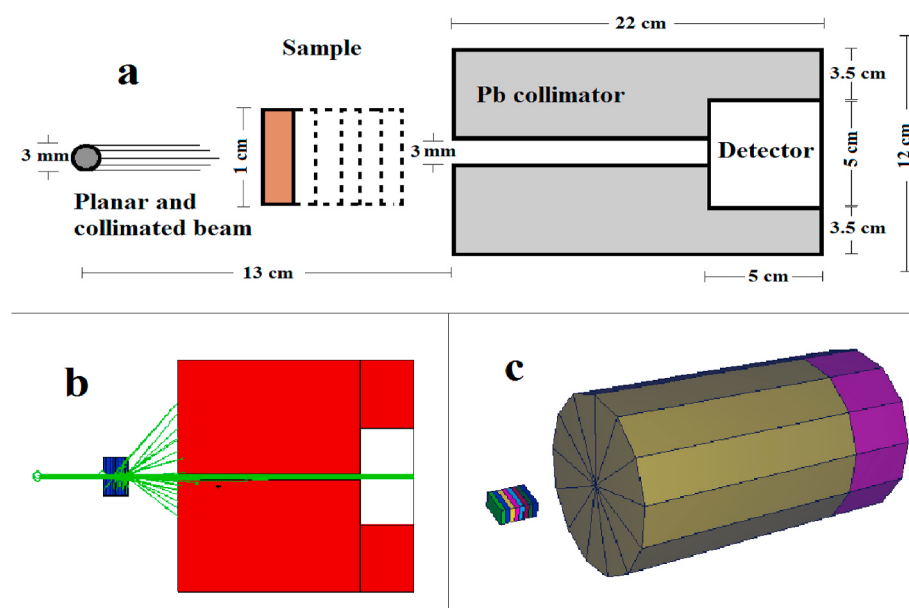
* Corresponding author.

E-mail addresses: reza_bagheri@aut.ac.ir, rzbagheri@aeoi.org.ir (R. Bagheri).

Table 1

Percentage (weight %) of atomic composition and densities of borate glass samples.

Element	Atomic number	BaO-glass (mol%)				Bi ₂ O ₃ -glass (mol%)				PbO-glass (mol%)			
		20	30	40	50	20	30	40	50	25	30	45	50
Oxygen	8	48.17	40.53	34.14	28.71	32.24	25.46	21.04	17.92	37.03	33.19	24.22	21.86
Boron	5	20.03	15.98	12.58	9.70	11.62	8.03	5.69	4.04	15.01	13.08	8.57	7.38
Barium	56	31.80	43.49	53.28	61.60	—	—	—	—	—	—	—	—
Lead	82	—	—	—	—	—	—	—	—	47.96	53.73	67.21	70.76
Bismuth	83	—	—	—	—	56.14	66.51	73.28	78.04	—	—	—	—
Density (g cm ⁻³)	—	—	3.490	—	—	3.948	4.554	4.958	5.306	3.487	3.870	4.468	4.658

**Fig. 1.** Geometry of modeled configuration. a: sizes are not on scale, b: particle track displaying (2-D view) and c: 3-D view of geometry.

calculated at the energy range of 10 keV to 10 MeV on the basis of the elemental composition of glass samples using version 2.6.0 of MCNPX code (Los Alamos National Laboratory, New Mexico, United States), XCOM (National Institute of Standards and Technology (NIST), Gaithersburg, Maryland, United States) and XMuDat programs (International Atomic Energy Agency (IAEA), Vienna, Austria) for first time. The Auto-Z_{eff} software and linear interpolation method were applied to determine the effective atomic number (Taylor et al., 2012). Also, efforts are put in to verify and validate the simulated and calculated values with the available experimental data.

The hypothesis of this research is to study the effect of added barium, bismuth and lead oxides on the radiation shielding properties of borate oxide glasses. Therefore, the obtained results will be discussed in terms of increased barium, bismuth and lead oxides contributions in the studied borate glass samples. The results of this study would probably be applicable in radiation shielding related topics of radiation applications in the energy regions of interest.

2. Materials and methods

2.1. Simulation

The MCNPX code is a general-purpose Monte Carlo radiation transport code for modeling the interaction of radiation with matter (Shultz and Faw, 2010). Cubical geometries were employed in this code for the modeling of glass samples. Using macrobody rectangular parallelepiped (RPP) card, eight sections of sub-rectangular cuboids, 0.05 cm–0.3 cm in thickness were considered for every type of sample and set on the z axis in tandem. Attenuation coefficients of the borate glass samples were

measured in a narrow beam transmission geometry using planar sources with collimated and monoenergetic beam that radiate gamma rays perpendicular to the front face of glass samples. A disk source of 0.3 cm diameter and parallel to the surface of the glasses was defined in a data card of MCNPX code with ERG, PAR, POS, AXS and DIR commands for energy, type of particle, position, reference vector and direction, respectively. The densities and the percentages by weight of each element in the glass samples used in the material card of MCNPX are presented in Table 1. Densities of glass samples were derived from Khanna et al. (1996) and Samdani et al. (2013) articles.

A small cylinder, 5 cm in diameter and 5 cm in length, was considered as the detector volume and set inside a lead collimator, with 12 cm and 0.3 cm outer and inner diameters, respectively. Tally F4 that calculates average flux in a cell (detector volume) was used to obtain simulation data. Fig. 1 shows the geometry of the system used for simulation. MCNP/MCNPX Visual Editor computer code of version X_24E was used for plotting of geometry and particles' tracks.

Simulations were performed with 100,000 to 1 million histories depending on the type and thickness of glass samples. In order to variance reduction of tally, the model geometry and the physics of the problem were simplified, and the main variance reduction technique of geometry splitting (using imp command) was applied for the transport of particles in the cells with a greater importance.

The 10 statistical checks for the estimated answer of tally in the tally fluctuation chart (tfc) bin of MCNPX output file, were passed for all simulations. All results were reported with less than 0.1% relative error and the decrease rate of relative error was as square root of histories. Figure of merit (FOM) value and its behavior were constant and random, respectively.

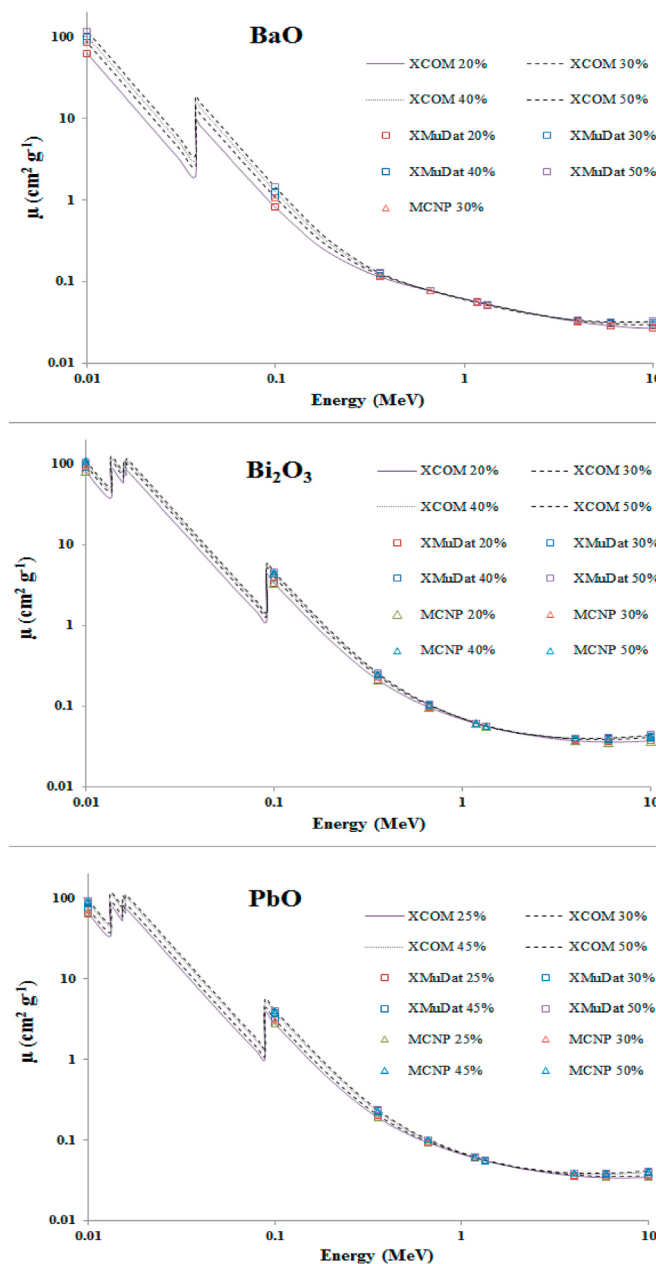


Fig. 2. Mass attenuation coefficients of $xR_mO_n:(100-x)B_2O_3$ glass system ($20 \leq x$ (mol%) ≤ 50).

Table 2
Absorption edges (in keV) of Pb, Bi and Ba above 10 keV.

Element	Z	L3	L2	L1	K
Pb	82	13.035	15.200	15.861	88.005
Bi	83	13.419	15.711	16.388	90.526
Ba	56	—	—	—	37.441

The MCPLIB04 photon transport library was used for the simulations in the MCNPX code. MCPLIB04 was officially released in 2002 (White, 2002). The cross section, form factor, and fluorescence data are all derived from the ENDF/B-VI.8 data library derived from EPDL97 (Cullen et al., 1997). Cross section data are given for incident photon energies from 1 keV to 100 GeV. Fluorescence data are adopted from the atomic relaxation data available in ENDF/B-VI.8 but use the storage and sampling scheme defined by Everett and Cashwell (1973).

2.2. Programs

The theoretical values for mass attenuation coefficients of the different elements, compounds and mixtures have been provided by Hubbell and Seltzer (1995) and Boone and Chavez (1996) and given in the form of XCOM and XMuDat programs by Gerward et al. (2004) and Nowotny (1998), respectively. In addition, Auto-Z_{eff} is user-friendly software which computes of the effective atomic numbers via exploitation of the smooth correlation between atomic cross section and atomic number (Taylor et al., 2012). This software surpasses dubious power-law approach. Therefore, XCOM and XMuDat programs as well as Auto-Z_{eff} software were used for the determination of shielding characteristics and for comparison with MCNPX results too.

2.3. Theory

Mass attenuation coefficients of glass samples (μ_m) were derived from transmission factors curves in various thicknesses of glass samples using Lambert's law which is described by the following equation (Sharifi et al., 2013):

$$I = I_0 e^{-\mu t} \quad (1)$$

where I_0 and I denote the incoming and outgoing intensities of photons through attenuator, t is sample thickness, and μ denotes the linear attenuation coefficient. In case of MCNPX code simulation, I and I_0 were considered in accordance with tally F4 values in output file, respectively in the presence of attenuator (glass samples) and without them, in order to extract linear attenuation coefficient of glasses from Eq. (1) and calculation of subsequent parameters. The mass attenuation coefficients (μ_m) were calculated by dividing linear attenuation coefficient of each glass sample by its density.

Additionally, the half value layer (HVL) quantity is defined as the extent of attenuator thickness, which reduce photon intensity to half of its initial value and is calculated using the following relation (Sharifi et al., 2013):

$$HVL = \frac{\ln 2}{\mu} \quad (2)$$

The effective atomic cross section (σ_a) of glass samples are calculated from simulation and calculation (XCOM and XMuDat) values of μ_m using the following relationship (Bagheri et al., 2017b):

$$\sigma_a = \frac{\mu_m}{N_A} \sum f_i A_i \quad (3)$$

where A_i is the atomic mass of the i th element and N_A is the Avogadro's number. Also f_i denotes the fractional abundance of the i th element with respect to the number of atoms such as $f_1+f_2+f_3+\dots+f_i=1$.

The linear interpolation method was applied to extract the Z_{eff} values from simulated and calculated values of mass attenuation coefficients. The procedure of calculating Z_{eff} by the interpolation method is to find the atomic number corresponding to the effective atomic cross section of the glass sample in a graph where, the variation of effective atomic cross section of the elements ($8 \leq Z \leq 83$) as a function of the atomic number, were shown for all studied photon energies.

Finally, the effective electron densities (N_{eff}) of glass samples are calculated from Eq. (3) (Bootjomchai et al., 2012):

$$N_{eff} = N_A \frac{Z_{eff}}{\sum f_i A_i} \quad (4)$$

3. Results and discussion

3.1. Mass attenuation coefficients and HVL values of glass samples

Mass attenuation coefficients of glass samples obtained by MCNPX

Table 3

HVL values (cm) of borate glass samples using the MCNPX code.

Photon energy (MeV)	BaO-glass (mol%)		Bi ₂ O ₃ -glass (mol%)			PbO-glass (mol%)				
	30	20	20	30	40	50	25	30	45	50
0.01	0.002		0.002	0.002	0.001	0.001	0.003	0.002	0.002	0.002
0.1	0.191		0.053	0.039	0.032	0.029	0.072	0.059	0.041	0.037
0.356	1.668		0.846	0.667	0.580	0.522	1.055	0.898	0.690	0.642
0.662	2.595		1.833	1.528	1.373	1.261	2.158	1.905	1.575	1.491
1.173	3.567		2.894	2.495	2.277	2.126	3.326	2.985	2.571	2.461
1.332	3.820		3.161	2.733	2.505	2.335	3.603	3.239	2.793	2.678
4	6.058		4.741	3.971	3.572	3.290	5.527	4.890	4.056	3.852
6	6.634		4.975	4.080	3.628	3.309	5.766	5.106	4.111	3.880
10	6.930		4.879	3.899	3.407	3.077	5.843	5.029	3.932	3.673
Density (g cm ⁻³)	3.490		3.948	4.554	4.958	5.306	3.487	3.870	4.468	4.658

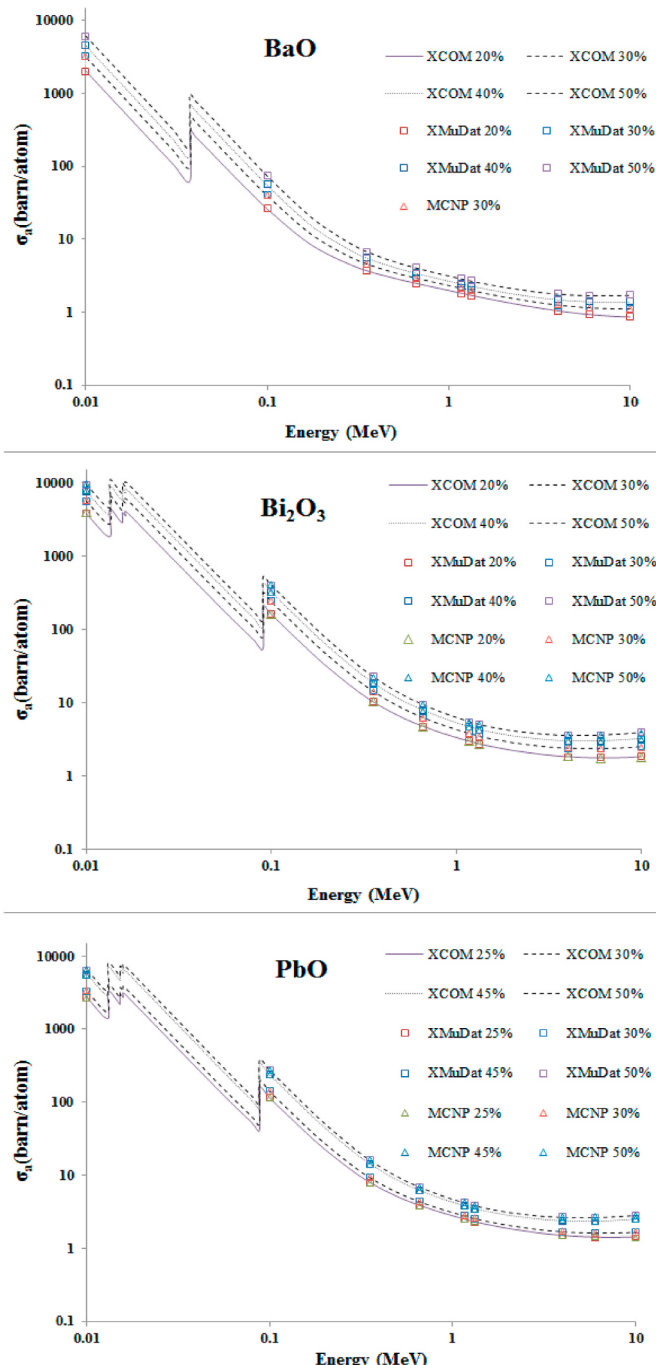
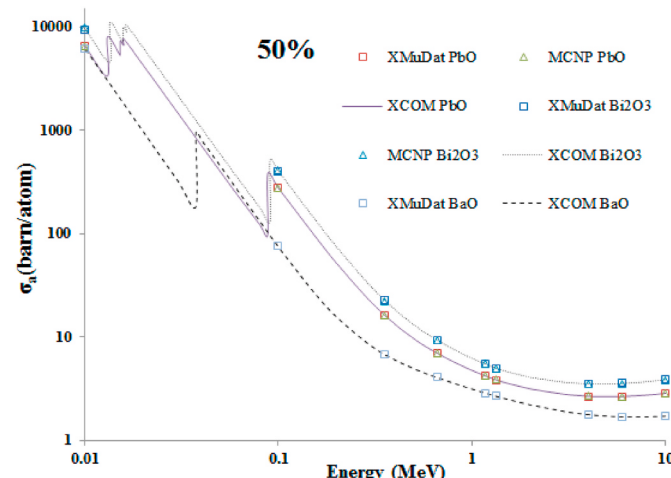


Fig. 3. Effective atomic cross sections (barn/atom) of borate glass samples.

Fig. 4. Effective atomic cross sections of 50R_mO_n:50B₂O₃ glass systems.

code, XCOM and XMudat programs for photon energies of interest in this research are shown in Fig. 2. A good agreement was observed between simulated and calculated values. As shown in Fig. 2, the μ_m values decrease with increase in the photon energy which beyond about 1 MeV these changes reduce and an extended smooth region appear. Multiple discontinuous peaks observed in the low photon energy region (0.01–0.1 MeV) of Fig. 2 for all three glass samples are K-, and L-photoelectric absorption edges of Ba, Bi and Pb elements, respectively. The related energies of these discontinuities are presented in Table 2 (Hubbell and Seltzer, 1995). Photoelectric absorption is responsible for these sudden increases in the mass attenuation coefficients of glass samples which happens right above the binding energy of the K and L shell electrons of the Ba, Bi and Pb atoms.

Also, Fig. 2 shows the dependency of μ_m of xR_mO_n:(100-x)B₂O₃ glass samples on mol% of BaO, Bi₂O₃, and PbO metal oxides. The μ_m values of the glass samples improve with increasing the Bi₂O₃, PbO and BaO concentrations, excluding the energy range of about 0.3–6 MeV, where the Compton Effect takes over as dominant process. The photoelectric and pair production effects are favored by high atomic number absorbers at low and high energy regions. It is seen that at energies which Compton Effect gradually predominates as the main interaction process, the μ_m values are almost independent of the atomic number of the constituent elements and their concentrations. Approximately, the 50Bi₂O₃:50B₂O₃ glass system had the highest mass attenuation coefficients at the most of the studied photon energy range.

The HVL values were determined using Eq. (2). The dependencies of the HVL values of the borate glass samples on photon energy are shown in Table 3. The HVL values of the glasses increase with the increase in photon energy and decrease with the increase in the density of glass samples. Additionally, it is obvious from Table 3 that Bi₂O₃-glass and

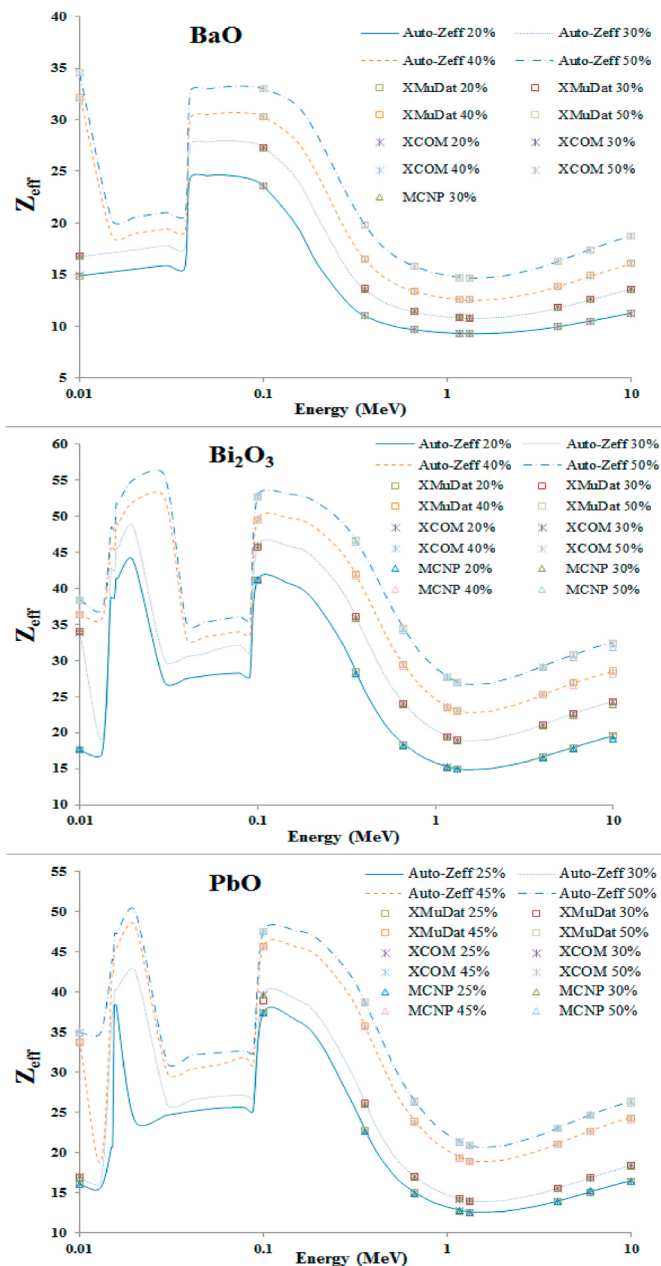


Fig. 5. Effective atomic numbers (Z_{eff}) of borate glasses.

especially 50Bi₂O₃:50B₂O₃ glass system have the lowest values of HVL at each photon energy. Therefore above mentioned glass system will have the highest shielding efficiency compared to other glasses.

3.2. Effective atomic cross section of glass samples

The effective atomic cross sections (σ_a) of glass samples are shown in Fig. 3. For all three glass samples, the σ_a values decrease as the photon energy increases. Unlike the μ_m values, the σ_a values of glass samples increase by increasing their BaO, Bi₂O₃ and PbO contents at any photon energy.

At the photon energies above 0.1 MeV, the σ_a values of glasses decrease in the following order: Bi₂O₃ ≥ PbO ≥ BaO (see Fig. 4). This is related to the weight fraction ratio of high atomic number elements (Bi, Pb, and Ba) in the three borate glass systems at a certain mol%. For 50% molar fraction, the weight% of Bi, Pb and Ba are 78.04, 70.76 and 61.60%, respectively.

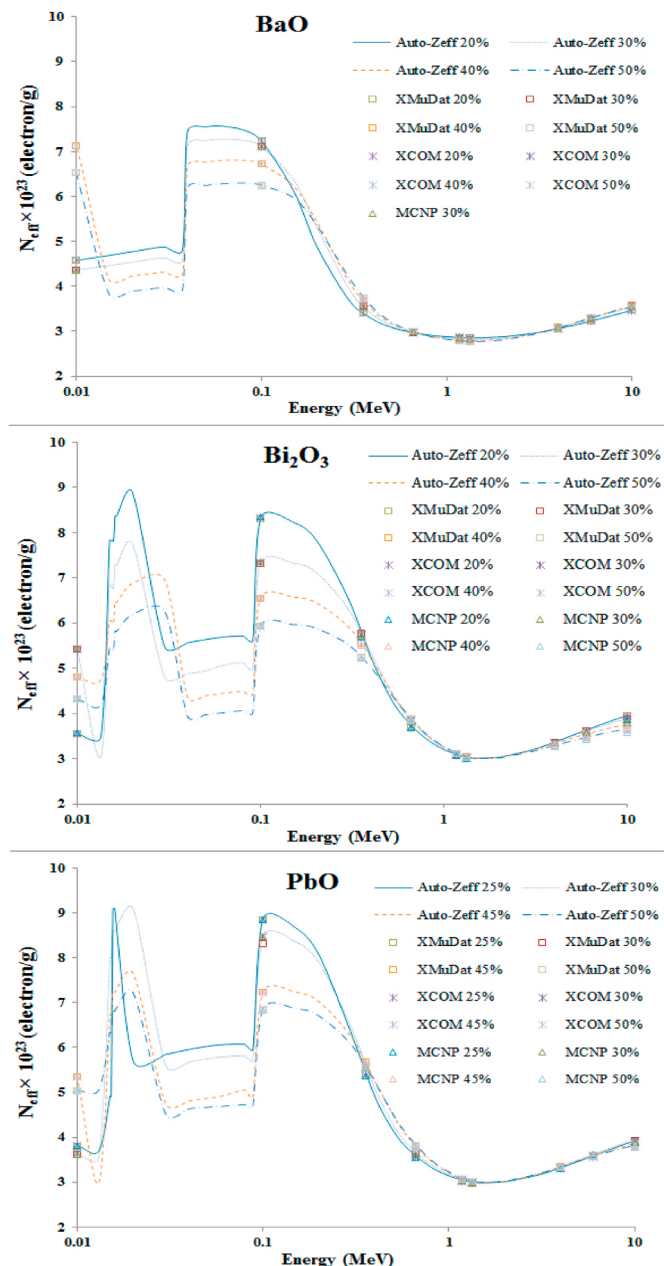


Fig. 6. Effective electron densities (N_{eff}) of borate glasses.

Below 0.1 MeV, it is seen several discontinuous jumps and disorders for the σ_a curves. These discontinuities mainly correspond to the K and L edges of bismuth, lead and barium elements (see Table 2). Due to photoelectric absorption edge of barium at 37.44 keV photon energy, σ_a curve of this borate glass shows a disorder and temporarily stands above lead oxide borate glass curve until K edges of lead reaches.

3.3. Effective atomic number and electron density of glass samples

The effective atomic numbers (Z_{eff}) and effective electron densities (N_{eff}) of borate glass samples based on the linear interpolation method were displayed in Figs. 5 and 6, respectively. The MCNPX, XCOM and XMuDat values along with the Auto-Zeff software results are shown.

The discontinuous jumps in low energy region (<100 keV) are related to photoelectric absorption edges of Ba, Bi and, Pb elements. Above 37.44, 88.01 and 90.53 keV for respectively, barium, lead and bismuth oxide borate glasses, the Z_{eff} and N_{eff} decreases rapidly with

Table 4Mass attenuation coefficients ($\times 10^{-2} \text{ cm}^2 \text{ g}^{-1}$) of studied glass systems at 662 keV photon energy.

No.	Sample	mol %	Density (g cm^{-3})	Method				
				XCOM	XMuDat	MCNPX	Experiment	RD%
1	$\text{xBaO:(1-x)B}_2\text{O}_3$	20	—	7.62	7.60	—	—	—
2		30	3.490 (Samdani et al., 2013)	7.65	7.63	7.65	—	—
3		40	—	7.67	7.65	—	—	—
4		50	—	7.69	7.67	—	—	—
5	$\text{xBi}_2\text{O}_3:(1-x)\text{B}_2\text{O}_3$	20	3.948 (Khanna et al., 1996)	9.64	9.61	9.58	9.70 ± 0.34 (Khanna et al., 1996)	-1.24
6		30	4.554 (Khanna et al., 1996)	10.02	10.00	9.96	9.71 ± 0.36 (Khanna et al., 1996)	3.19
7		40	4.958 (Khanna et al., 1996)	10.28	10.25	10.18	9.97 ± 0.28 (Khanna et al., 1996)	3.11
8		50	5.306 (Khanna et al., 1996)	10.45	10.43	10.36	9.96 ± 0.33 (Khanna et al., 1996)	4.92
9	$\text{xPbO:(1-x)B}_2\text{O}_3$	25	3.487 (Khanna et al., 1996)	9.21	9.2	9.21	8.36 ± 0.30 (Khanna et al., 1996)	10.17
10		30	3.870 (Khanna et al., 1996)	9.41	9.4	9.40	8.80 ± 0.25 (Khanna et al., 1996)	6.93
11		45	4.468 (Khanna et al., 1996)	9.88	9.87	9.85	9.03 ± 0.19 (Khanna et al., 1996)	9.41
12		50	4.658 (Khanna et al., 1996)	10.01	9.99	9.98	9.21 ± 0.16 (Khanna et al., 1996)	8.69
16	Window glass	—	2.579 (Vascott and Seward, 2005)	7.69	7.68	7.74	—	—
17	Ordinary concrete	—	2.30 (Sharifi et al., 2013)	7.88	—	7.93	8.09 (Sharifi et al., 2013)	-2.60
18	Barite concrete	—	3.35 (Akkurt et al., 2010)	7.75	—	7.76	7.56 (Akkurt et al., 2010)	2.65
19	xBaO:(1-x)SiO_2	21	3.454 (Kirdsiri et al., 2011)	7.74	7.72	7.74	7.81 ± 0.15 (Kirdsiri et al., 2011)	-1.15
20	$\text{xBi}_2\text{O}_3:(1-x)\text{SiO}_2$	23	5.701 (Kirdsiri et al., 2011)	9.94	9.92	9.86	9.51 ± 0.38 (Kirdsiri et al., 2011)	4.52
21	xPbO:(1-x)SiO_2	45	5.601 (Singh et al., 2008)	10.02	10.00	9.98	10.40 (Singh et al., 2008)	-4.04
22	$\text{xBaO:(1-x)P}_2\text{O}_5$	28	—	7.67 (Bagheri and Adeli, 2020)	7.65 (Bagheri and Adeli, 2020)	—	—	...
23	$\text{xBi}_2\text{O}_3:(1-x)\text{P}_2\text{O}_5$	31	—	9.59 (Bagheri and Adeli, 2020)	9.56 (Bagheri and Adeli, 2020)	—	—	0.84
24	$\text{xPbO:(1-x)P}_2\text{O}_5$	49	4.8 (Kharita et al., 2012)	9.52	9.50	9.49	8.75 (Kharita et al., 2012)	8.80

photon energy increase in a region with Compton Effect dominance and begin to rise gradually at the pair production region. Also, Figs. 5 and 6 show while the Z_{eff} values of the glass samples improve with the increase in their Bi_2O_3 , PbO and BaO contents, increasing these contents to the same fraction has no significant effect on N_{eff} of borate glasses. The $50\text{Bi}_2\text{O}_3:50\text{B}_2\text{O}_3$ glass system had the highest Z_{eff} value of 55.60 at the 30 keV photon energy. The N_{eff} values of the studied glass systems varied in the range of $2.77 \times 10^{23} - 9.10 \times 10^{23}$ electron/g.

3.4. Comparison with available experimental data

In order to verify and validate the simulated and calculated values, the μ_m values of studied borate glasses were compared with available experimental data in Table 4. In addition, it was tried to compare the shielding property of borate based glasses with silicate and phosphate based glasses as well as with some standard shielding glasses and concretes from literature.

As seen in Table 4, a good agreement is observed between the simulated and calculated values with experimental data. The relative deviation (RD: differences between simulated and calculated results with the experimental data) are less than $\pm 11\%$. The MCNPX results showed better agreement with the experimental data. Also, the reported experimental errors are in the range of $\leq \pm 3.7\%$ (Khanna et al., 1996). For all of the three barium oxide glass systems (borate, silicate, and phosphate), the μ_m values are within the limits of window glass, ordinary and barite concretes. The bismuth and lead oxides glass systems exhibit better shielding properties than barite concrete as an appropriate high-density shielding concrete. Also, Table 4 shows that at equal concentrations of additives (BaO , Bi_2O_3 , PbO), the silicate glass sample contains the higher values of μ_m in comparison with phosphate and

borate glasses. It should be noted that the differences in the used geometry of simulation relative to experimental geometries lead to little discrepancy in calculation and measured values.

4. Conclusion

Gamma-ray shielding properties of borate glasses (μ_m , HVL, σ_a , Z_{eff} and N_{eff}) containing different concentrations of BaO , Bi_2O_3 , and PbO were studied at 10 keV–10 MeV photon energies using MCNPX code, XCOM and XMuDat computer programs and Auto-Z_{eff} software and linear interpolation method exclusively for Z_{eff} calculations. It was found that the results by simulation, calculation, and the experiment are in good agreement with each other (within $\pm 10.17\%$). Except for the energy range of 0.3–6 MeV (Compton Effect territory), μ_m values of glass samples improved by increasing their BaO , PbO and Bi_2O_3 contents. However, the σ_a and Z_{eff} values of glasses increased by increasing their metal oxides contents at the studied range of photon energy. Furthermore, HVL values of glasses increased with the photon energy increase while the μ_m and σ_a values decreased. Above 0.4 MeV photon energy, N_{eff} values were independent of the metal oxides contents.

The results demonstrated that the $50\text{Bi}_2\text{O}_3:50\text{B}_2\text{O}_3$ glass sample of high density (5.306 g cm^{-3}) and with constituents of high-atomic-number elements is a more effective shield relative to other studied glass samples. This glass system had the highest Z_{eff} value of 55.60 at the 30 keV photon energy and the lowest value of HVL in each studied photon energy. This study indicates that MCNPX code and applied computer programs provides reliable values of gamma-ray shielding characteristics for borate glass systems. The results of this study would probably be applicable in radiation dosimetry, health physics, shielding related topics, nuclear medicine and radiation therapy, diagnostics,

conservation and sterilization of food and other radiation applications in the energy regions of interest.

Author statement

Reza Bagheri: Conceptualization, Writing- Original draft, Methodology, Reviewing and Editing, Simulation, Investigation. Seyed Pezhman Shirmardi: Reviewing and Editing, Investigation, Simulation.

Declaration of competing interest

The authors declare that they have no known competing financial interests or personal relationships that could have appeared to influence the work reported in this paper.

References

- Abouhaswa, A.S., El-Mallawany, R., Rammah, Y.S., 2020. Direct influence of La on structural, optical and gamma ray shielding of lead borate glasses. *Radiat. Phys. Chem.* 177, 109085.
- Akkurt, I., Akyildirim, H., Mavi, B., Kilincarslan, S., Basyigit, C., 2010. Photon attenuation coefficients of concrete include barite in different rate. *Ann. Nucl. Energy* 37, 910–914.
- Akkurt, I., Tekin, H.O., 2020. Radiological parameters for bismuth oxide glasses using Phy-X/PSD software. *Emerg. Mater. Res.* 9, 1020–1027.
- Al-Buraihi, M.S., Sriwunkum, C., Arslan, H., et al., 2020. Investigation of barium borate glasses for radiation shielding applications. *Appl. Phys. A* 126, 1–9.
- Al-Hadeethi, Y., Sayyed, M.I., Agar, O., 2020a. Ionizing photons attenuation characterization of quaternary tellurite-zinc-niobium-gadolinium glasses using Phy-X/PSD software. *J. Non-Cryst. Solids* 538, 120044.
- Al-Hadeethi, Y., Sayyed, M.I., Mohammed, H., Rimondin, L., 2020b. X-ray photons attenuation characteristics for two tellurite based glass systems at dental diagnostic energies. *Ceram. Int.* 46, 2551–257.
- Al-Hadeethi, Y., Sayyed, M.I., Rammah, Y.S., 2020c. Fabrication, optical, structural and gamma radiation shielding characterizations of $\text{GeO}_2\text{-PbO}\text{-Al}_2\text{O}_3\text{-CaO}$ glasses. *Ceram. Int.* 46, 2055–2062.
- Bagheri, R., Adeli, R., 2020. Gamma-ray shielding properties of phosphate glasses containing Bi_2O_3 , PbO , and BaO in different rates. *Radiat. Phys. Chem.* 174, 108918.
- Bagheri, R., Moghaddam, A.K., Shirmardi, S.P., Azadbakht, B., Salehi, M., 2018. Determination of gamma-ray shielding properties for silicate glasses containing Bi_2O_3 , PbO , and BaO . *J. Non-Cryst. Solids* 479, 62–71.
- Bagheri, R., Moghaddam, A.K., Yousefnia, H., 2017a. Gamma ray shielding study of barium-bismuth-borosilicate glasses as transparent shielding materials using MCNP-4C code, XCOM program, and available experimental data. *Nucl. Eng. Technol.* 49, 216–223.
- Bagheri, R., Shirmardi, S.P., Adeli, R., 2017b. Study on gamma-ray shielding characteristics of lead oxide, barite, and boron ores using MCNP-4C Monte Carlo code and experimental data. *J. Test. Eval.* 45, 2259–2266.
- Boone, J.M., Chavez, A.E., 1996. Comparison of X-ray cross sections for diagnostic and therapeutic medical physics. *Med. Phys.* 23, 1997–2005.
- Bootjomchai, C., Laopaiboon, J., Yenchai, C., Laopaiboon, R., 2012. Gamma-ray shielding and structural properties of barium-bismuth-borosilicate glasses. *Radiat. Phys. Chem.* 81, 785–790.
- Cullen, D.E., Hubbel, J.H., Kissel, L.D., 1997. EPDL97: the Evaluated Photon Data Library, 97 Version. In: UCRL-50400, vol. 6. Lawrence Livermore National Laboratory, Livermore, CA. Rev 5.
- Everett, C.J., Cashwell, E.D., 1973. MCP Code Fluorescence Routine Discussion, Report LA-5240-MS. Los Alamos National Laboratory, Los Alamos, NM.
- Gerward, L., Gilbert, N., Jensen, K.B., Levring, H., 2004. WinXCom—A program for calculating X-ray attenuation coefficients. *Radiat. Phys. Chem.* 71, 653–654.
- Hubbell, J.H., Seltzer, S.M., 1995. Tables of X-Ray Mass Attenuation Coefficients and Mass Energy-Absorption Coefficients 1 keV–20 MeV for Elements 1 < Z < 92 and 48 Additional Substances of Dosimetric Interest. National Institute of Standards and Physics Laboratory. NISTIR 5632.
- Kaky, K.M., Sayyed, M.I., Mhareb, M.H.A., Abdalsalam, A.H., Mahmoud, K.M., Baki, S.O., Mahdi, M.A., 2020. Physical, structural, optical and gamma radiation attenuation properties of germinate-tellurite glasses for shielding applications. *J. Non-Cryst. Solids* 545, 120250.
- Khanna, A., Bhatti, S.S., Singh, K.J., Thind, K.S., 1996. Gamma-ray attenuation coefficients in some heavy metal oxide borate glasses at 662 keV. *Nucl. Instrum. Methods B* 114, 217–220.
- Kharita, M.H., Jabra, R., Yousef, S., Samaan, T., 2012. Shielding properties of lead and barium phosphate glasses. *Radiat. Phys. Chem.* 81, 1568–1571.
- Kirdsiri, K., Kaewkhao, J., Chanthima, N., Limsuwan, P., 2011. Comparative study of silicate glasses containing Bi_2O_3 , PbO and BaO : radiation shielding and optical properties. *Ann. Nucl. Energy* 38, 1438–1441.
- Kumar, A., Gaikwad, D.K., Obaid, S.S., Tekin, H.O., Agar, O., Sayyed, M.I., 2020. Experimental studies and Monte Carlo simulations on gamma ray shielding competence of $(30+x)\text{PbO}-10\text{WO}_3-10\text{Na}_2\text{O}-10\text{MgO}-(40-x)\text{B}_2\text{O}_3$ glasses. *Prog. Nucl. Energy* 119, 103047.
- Nowotny, R., 1998. XMuDat: photon attenuation data on PC. In: Tech. Rep. IAEA-NDS-195. International Atomic Energy Agency, Vienna.
- Obaid, S.S., Sayyed, M.I., Gaikwad, D.K., Pawar, P.P., 2018a. Attenuation coefficients and exposure buildup factor of some rocks for gamma ray shielding applications. *Radiat. Phys. Chem.* 148, 86–94.
- Obaid, S.S., Sayyed, M.I., Gaikwad, D.K., Tekin, H.O., Elmahrour, Y., Pawar, P.P., 2018b. Photon attenuation coefficients of different rock samples using MCNPX, Geant4 simulation codes and experimental results: a comparison study. *Radiat. Eff. Defect Solid* 173, 900–914.
- Saddeek, Y.B., Tekin, H.O., Issa, S.A.M., Kilicoglu, O., Elshami, W., Alharbi, T., 2020. An in-depth investigation from mechanical durability to structural and nuclear radiation attenuation properties: $\text{B}_2\text{O}_3\text{-Na}_2\text{O}\text{-Bi}_2\text{O}_3\text{-Nb}_2\text{O}_5$ glasses experience. *Phys. Scripta* 95, 105701.
- Samdani, Shareefuddin, Md, Ramadevudu, G., Rao, S.L.S., Chary, M.N., 2013. Physical, optical, and spectroscopic studies on $\text{MgO}\text{-BaO}\text{-B}_2\text{O}_3$ glasses. *ISRN Ceram.* 2013, 1–11, 2013.
- Sayyed, M.I., Agar, O., Kumar, A., Tekin, H.O., Gaikwad, D.K., Obaid, S.S., 2020a. Shielding behaviour of $(20+x)\text{Bi}_2\text{O}_3-20\text{BaO}-10\text{Na}_2\text{O}-10\text{MgO}-(40-x)\text{B}_2\text{O}_3$: an experimental and Monte Carlo study. *Chem. Phys.* 529, 110571.
- Sayyed, M.I., Kumar, A., Tekin, H.O., et al., 2020b. Evaluation of gamma-ray and neutron shielding features of heavy metals doped $\text{Bi}_2\text{O}_3\text{-BaO-Na}_2\text{O-MgO-B}_2\text{O}_3$ glass systems. *Prog. Nucl. Energy* 118, 103118.
- Sayyed, M.I., Tekin, H.O., Agar, O., 2019. Gamma photon and neutron attenuation properties of $\text{MgO}\text{-BaO}\text{-B}_2\text{O}_3\text{-TeO}_2\text{-Cr}_2\text{O}_3$ glasses: the role of TeO_2 . *Radiat. Phys. Chem.* 163, 58–66.
- Sayyed, M.I., Tekin, H.O., Altunsoy, E.E., Obaid, S.S., Almatari, M., 2018. Radiation shielding study of tellurite tungsten glasses with different antimony oxide as transparent shielding materials using MCNPX code. *J. Non-Cryst. Solids* 498, 167–172.
- Sharifi, S., Bagheri, R., Shirmardi, S.P., 2013. Comparison of shielding properties for ordinary, barite, serpentine and steel-magnetite concretes using MCNP-4C code and available experimental results. *Ann. Nucl. Energy* 53, 529–534.
- Shultzis, J.K., Faw, R.E., 2010. An MCNP Premier. Department of Mechanical and Nuclear Engineering, Kansas State University.
- Singh, K.J., Singh, N., Kaundal, R.S., Singh, K., 2008. Gamma-ray shielding and structural properties of PbO-SiO_2 glasses. *Nucl. Instrum. Methods B* 266, 944–948.
- Singh, V.P., Ali, A.M., Badiger, N.M., El-Khayatt, A.M., 2013. Monte Carlo simulation of gamma ray shielding parameters of concretes. *Nucl. Eng. Des.* 265, 1071–1077.
- Susoy, G., Altunsoy Guclu, E.E., Kilicoglu, O., Kamislioglu, M., Al-Buraihi, M.S., Abuzaid, M.M., Tekin, 2020. The impact of Cr_2O_3 additive on nuclear radiation shielding properties of $\text{LiF-SrO-B}_2\text{O}_3$ glass system. *Mater. Chem. Phys.* 242, 122481.
- Taylor, M.L., Smith, R.L., Dossing, F., Franich, R.D., 2012. Robust calculation of effective atomic numbers: the Auto-Z_{eff} software. *Med. Phys.* 39, 1769–1778.
- Tekin, H.O., Issa, S.A.M., Mahmoud, K.A.A., et al., 2020a. Nuclear radiation shielding competencies of barium-reinforced borosilicate glasses. *Emerg. Mater. Res.* 9, 1131–1144.
- Tekin, H.O., Kassab, L.R.P., Issa, S.A.M., Martins, M.M., Bontempo, L., da Silva Mattos, G.R., 2020b. Newly developed BGO glasses: synthesis, optical and nuclear radiation shielding properties. *Ceram. Int.* 46, 11861–11873.
- Vascott, T., Seward III, T.P., 2005. High Temperature Glass Melt Property Database for Process Modeling, 1 edition. Wiley-American Ceramic Society Publication, Westerville, Ohio.
- White, M.C., 2002. Photoatomic Data Library MCPLIB04: A New Photoatomic Library Based on Data from ENDF/B-VI Release 8, Internal Memorandum X-5: MCW-02-111. Los Alamos National Laboratory, Los Alamos, NM.
- Yasmin, B.S., Barua, M.U., Khandaker, M.A., Chowdhury, F.U.Z., Abdur Rashid, Md, Bradley, D.A., Olatunji, M.A., Kamal, M., 2018. Studies of ionizing radiation shielding effectiveness of silica-based commercial glasses used in Bangladeshi dwellings. *Results Phys.* 9, 541–549.